

SUPPLEMENT TO “THE LUCAS ORCHARD”
 (*Econometrica*, Vol. 81, No. 1, January 2013, 55–111)

BY IAN MARTIN

FIGURE S.1 shows the functions $\mathcal{F}_\gamma(z)$, scaled by 2^γ so that they integrate to 1.

S.1. SIMPLE SPECIAL CASES WITH SYMMETRIC BROWNIAN MOTIONS

In some special cases, it is possible to obtain considerably simpler expressions for the price-dividend ratio. In this section, I consider the special case in which the log dividend processes of each asset follow independent drifting Brownian motions with drifts μ and volatilities σ . It follows that the CGF is given by

$$(S.1) \quad \mathbf{c}(\theta_1, \theta_2) = \mu(\theta_1 + \theta_2) + \frac{1}{2}\sigma^2(\theta_1^2 + \theta_2^2).$$

Recall the general pricing formula,

$$\frac{P_\alpha}{D_\alpha} = [2 \cosh(u/2)]^\gamma \cdot \int_{-\infty}^{\infty} \frac{e^{iuz} \mathcal{F}_\gamma(z)}{\rho - \mathbf{c}(\alpha_1 - \gamma/2 - iz, \alpha_2 - \gamma/2 + iz)} dz.$$

I focus on pricing the claim to asset 1, so $\alpha_1 = 1, \alpha_2 = 0$. Substituting in from (S.1),

$$\rho - \mathbf{c}(1 - \gamma/2 - iz, -\gamma/2 + iz) = \sigma^2[(z + i/2)^2 + A^2],$$

where $A^2 \equiv (\rho + \mu(\gamma - 1))/\sigma^2 - (\gamma - 1)^2/4$. The finiteness condition requires that

$$\rho - \mathbf{c}(1 - \gamma/2, -\gamma/2) > 0 \quad \text{and} \quad \rho - \mathbf{c}(1 - \gamma, 0) > 0,$$

which amounts to the requirement that $A > (\gamma - 1)/2$.

The general pricing formula gives the price-dividend ratio of asset 1, written P/D_1 , as

$$(S.2) \quad P/D_1 = [2 \cosh(u/2)]^\gamma \cdot \int_{-\infty}^{\infty} \frac{e^{iuz} \mathcal{F}_\gamma(z)}{\sigma^2[(z + i/2)^2 + A^2]} dv.$$

The question, as before, is where the poles of the integrand are. In the upper half-plane, $\mathcal{F}_\gamma(z)$ has infinitely many regularly spaced poles on the imaginary axis, at $(\gamma/2)i, (\gamma/2 + 1)i, (\gamma/2 + 2)i, \dots$. The other pole is at the zero, in the upper half-plane, of the denominator $\sigma^2[(z + i/2)^2 + A^2]$ —that is, at $(A - 1/2)i$. It turns out that the integral takes on a relatively simple form if we ensure that the pole at $(A - 1/2)i$ is an integer distance from the poles $(\gamma/2)i$,

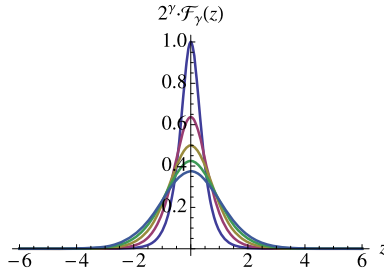


FIGURE S.1.—The functions $2^\gamma \cdot \mathcal{F}_\gamma(z)$ for $\gamma = 1$ (most peaked), 2, 3, 4, 5 (least peaked).

$(\gamma/2 + 1)i$, etc. (The simple example presented in Cochrane, Longstaff, and Santa-Clara (2008) has $\rho = \sigma^2$, so $A = 1$.) Thus, we want

$$A \in \{(\gamma + 1)/2, (\gamma + 3)/2, (\gamma + 5)/2, \dots\}.$$

For example, if $\gamma = 2$ and ρ is chosen so that $A = (\gamma + 1)/2 = 3/2$, the price-dividend ratio of asset 1 is

$$P/D_1(s) = \frac{2(1-s)^3 \log(1-s) + 2s - 5s^2 + 3s^3 - s^3 \log s}{3(1-s)^2 s^3 \sigma^2}.$$

In terms of the expression provided in Proposition 4 of the paper, these parameter choices correspond to choosing λ_1 and λ_2 so that the hypergeometric functions simplify nicely. In the symmetric independent case, setting $A = (\gamma + 1)/2$ implies that $\lambda_1 = \gamma/2$ and $\lambda_2 = -(1 + \gamma)/2$. These values give special cases of the hypergeometric functions that simplify in terms of more elementary functions, as above.

S.2. A MORE DETAILED BETA DECOMPOSITION

This section conducts a beta decomposition in more detail than was possible in the body of the paper. In the body of the paper, we considered the decomposition

$$(S.3) \quad \underbrace{\frac{\text{cov}_t(d \log P_1, d \log P_M)}{\text{var}_t d \log P_M}}_{\text{CAPM beta, } \beta} = \underbrace{\frac{\text{cov}_t(d \log D_1, d \log P_M)}{\text{var}_t d \log P_M}}_{\beta_{CF1}} + \underbrace{\frac{\text{cov}_t\left(d \log \frac{P_1}{D_1}, d \log P_M\right)}{\text{var}_t d \log P_M}}_{\beta_{DR1}},$$

as in Campbell and Mei (1993). Figures S.2(d) and S.2(g) show β_{CF1} and β_{DR1} in the model; they add up to CAPM beta, plotted in Figure S.2(a).

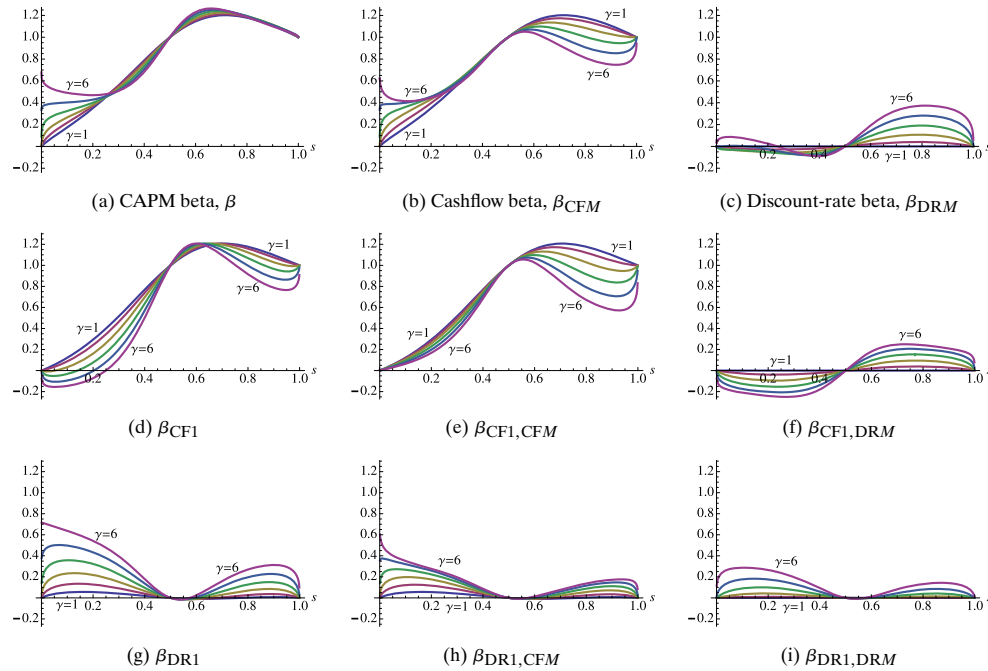


FIGURE S.2.—Beta decomposition. Panels in the top row are the sum of the panels below them. Panels in the left column are the sum of the panels to their right.

We also sliced the CAPM beta up in a different way, splitting the *market's* return into a cashflow component and a valuation component:

$$(S.4) \quad \underbrace{\frac{\text{cov}_t(d \log P_1, d \log P_M)}{\text{var}_t d \log P_M}}_{\text{CAPM beta}} = \underbrace{\frac{\text{cov}_t(d \log P_1, d \log C)}{\text{var}_t d \log P_M}}_{\text{cashflow beta, } \beta_{CFM}} + \underbrace{\frac{\text{cov}_t\left(d \log P_1, d \log \frac{P_M}{C}\right)}{\text{var}_t d \log P_M}}_{\text{discount-rate beta, } \beta_{DRM}}.$$

Cashflow beta measures the covariance of the asset's return with shocks to the aggregate market's cashflows, while discount-rate beta measures the covariance of the asset's return with shocks to the aggregate market's valuation ratio. This is the continuous-time version of the good-beta/bad-beta decomposition of Campbell and Vuolteenaho (2004). In a log-linear approximation of a homoskedastic conditionally lognormal model, Campbell (1993) derived an ICAPM result whose continuous-time analogue is that

$$(S.5) \quad \text{RP} = \gamma \sigma^2 \beta_{CFM} + \sigma^2 \beta_{DRM},$$

where RP_1 denotes asset 1's instantaneous risk premium, σ^2 is the instantaneous variance of the market return, and β_{CFM} and β_{DRM} were defined in (S.4). Figure S.3 shows that this holds to high accuracy in the present calibration. Figures S.2(b) and S.2(c) plot cashflow beta and discount-rate beta against s ; they add up to Figure S.2(a) to their left.

We can now complete the square by combining (S.3) and (S.4), splitting the returns on both asset 1 *and* the market into cashflow and discount-rate components. (Campbell, Polk, and Vuolteenaho (2010) carried out this exercise.) Doing so, we see that cashflow betas are high for a small asset because the small asset's *valuation ratio* covaries strongly with the market's cashflows (Figures S.2(e) and S.2(h), which add up to Figure S.2(b)). The picture is more mixed regarding a small asset's discount-rate beta. There are two forces pulling in opposite directions: a small asset's *cashflows* covary negatively with the market valuation ratio, but its *valuation ratio* covaries positively with the market valuation ratio (Figures S.2(f) and S.2(i), which add up to Figure S.2(c)).

S.3. CGFS FOR SECTION 3.1

Examples 1 through 3 do not have jumps. The CGF in each case is

$$\mathbf{c}(\boldsymbol{\theta}) = \boldsymbol{\mu}'\boldsymbol{\theta} + \frac{1}{2}\boldsymbol{\theta}'\boldsymbol{\Sigma}\boldsymbol{\theta}.$$

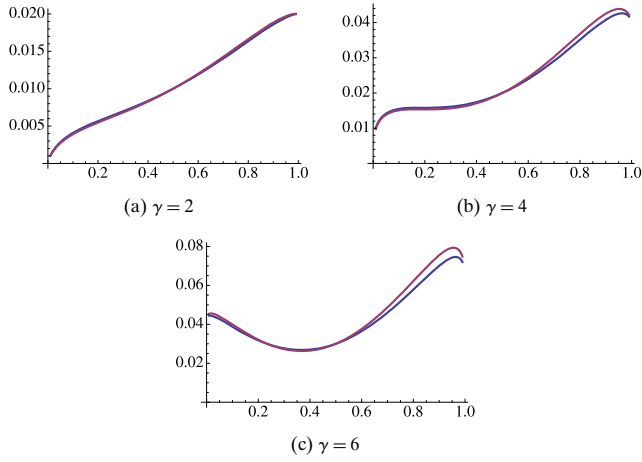


FIGURE S.3.—The exact excess return on asset 1 plotted against its share s (blue); and the excess return predicted by the continuous-time analogue of Campbell and Vuolteenaho's equation (8) (red).

In Examples 1 and 2, there are $N = 4$ assets, so $\boldsymbol{\theta}$ and $\boldsymbol{\mu}$ are four-dimensional vectors and $\boldsymbol{\Sigma}$ is a 4×4 matrix. In Example 3, there are $N = 5$ assets, so $\boldsymbol{\theta}$ and $\boldsymbol{\mu}$ are five-dimensional vectors and $\boldsymbol{\Sigma}$ is a 5×5 matrix.

In Example 1, we have

$$\boldsymbol{\mu} = \begin{pmatrix} 0.03 \\ 0.01 \\ 0.03 \\ 0.01 \end{pmatrix} \quad \text{and} \quad \boldsymbol{\Sigma} = \begin{pmatrix} 0.1^2 & 0 & 0 & 0 \\ 0 & 0.1^2 & 0 & 0 \\ 0 & 0 & 0.1^2 & 0 \\ 0 & 0 & 0 & 0.1^2 \end{pmatrix}.$$

In Example 2, we have

$$\boldsymbol{\mu} = \begin{pmatrix} 0.02 \\ 0.02 \\ 0.02 \\ 0.02 \end{pmatrix} \quad \text{and} \quad \boldsymbol{\Sigma} = \begin{pmatrix} 0.05^2 & 0 & 0 & 0 \\ 0 & 0.15^2 & 0 & 0 \\ 0 & 0 & 0.05^2 & 0 \\ 0 & 0 & 0 & 0.15^2 \end{pmatrix}.$$

In Example 3, we have

$$\boldsymbol{\mu} = \begin{pmatrix} 0.02 \\ 0.02 \\ 0.02 \\ 0.02 \\ 0.02 \end{pmatrix}$$

and

$$\Sigma = \begin{pmatrix} 0.1^2 & 0 & 0 & 0 & 0 \\ 0 & 0.1^2 & 0 & 0 & 0.5 \times 0.1^2 \\ 0 & 0 & 0.1^2 & 0 & 0 \\ 0 & 0 & 0 & 0.1^2 & 0.5 \times 0.1^2 \\ 0 & 0.5 \times 0.1^2 & 0 & 0.5 \times 0.1^2 & 0.1^2 \end{pmatrix}.$$

Example 4 features jumps. The CGF is

$$\mathbf{c}(\boldsymbol{\theta}) = \boldsymbol{\mu}'\boldsymbol{\theta} + \frac{1}{2}\boldsymbol{\theta}'\Sigma\boldsymbol{\theta} + \tilde{\omega}(e^{\boldsymbol{\mu}_j'\boldsymbol{\theta} + (1/2)\boldsymbol{\theta}'\Sigma_j\boldsymbol{\theta}} - 1),$$

where

$$\boldsymbol{\mu} = \begin{pmatrix} 0.02 \\ 0.02 \\ 0.02 \\ 0.02 \\ 0.02 \end{pmatrix} \quad \text{and} \quad \Sigma = \begin{pmatrix} 0.1^2 & 0 & 0 & 0 & 0 \\ 0 & 0.1^2 & 0 & 0 & 0 \\ 0 & 0 & 0.1^2 & 0 & 0 \\ 0 & 0 & 0 & 0.1^2 & 0 \\ 0 & 0 & 0 & 0 & 0.1^2 \end{pmatrix}$$

control the Brownian components, and $\tilde{\omega} = 0.017$ is the jump arrival rate, and

$$\boldsymbol{\mu}_j = \begin{pmatrix} 0 \\ -0.38 \\ 0 \\ -0.38 \\ -0.38 \end{pmatrix} \quad \text{and} \quad \Sigma_j = \begin{pmatrix} 0 & 0 & 0 & 0 & 0 \\ 0 & 0.25^2 & 0 & 0.25^2 & 0.25^2 \\ 0 & 0 & 0 & 0 & 0 \\ 0 & 0.25^2 & 0 & 0.25^2 & 0.25^2 \\ 0 & 0.25^2 & 0 & 0.25^2 & 0.25^2 \end{pmatrix}$$

control the distribution of disasters.

S.4. UNDERREACTION VERSUS COMOVEMENT

In the three-tree example of Section 3, the simplex can be divided into three regions. If asset 1 is sufficiently dominant, it overreacts to own-cashflow news, and other assets comove positively with it; at the other extreme, if asset 1 is sufficiently small, it underreacts to own-cashflow news, and other assets comove negatively; in between, asset 1 underreacts to own-cashflow news and other assets comove positively with it. This last regime applies when all three assets are the same size, in the middle of the simplex, where the riskless rate is constant to first order.

It is natural to ask what happens for larger N . How large must asset 1 be for other assets to comove with it? And how large must it be to overreact to its own cashflow news? In the $N = 2$ case, comovement and overreaction are intertwined: in a symmetric calibration, if an asset experiences overreaction when its share is larger than \bar{s} —where \bar{s} is the point at which $P_1/D_1(s)$ achieves its minimum, $\bar{s} = 0.608$ in the present calibration—then other assets will comove with it when its share is larger than $1 - \bar{s}$.

TABLE S.I
 REGIONS IN WHICH (POSITIVE) COMOVEMENT AND
 OVERREACTION OCCUR

N	Comovement if...		Overreaction if...	
	$s_1 \geq$	rel. size \geq	$s_1 \geq$	rel. size \geq
2	0.39	0.64	0.61	1.54
3	0.26	0.71	0.47	1.80
4	0.20	0.74	0.41	2.06
5	0.16	0.75	0.37	2.34
6	0.13	0.76	0.35	2.66

This tight link between overreaction and positive comovement is broken if $N \geq 3$. Table S.I shows the corresponding results for N up to 6, with $\gamma = 4$ and ρ set so that the long rate is 7%. In each case, I assume that asset 1 has dividend share s_1 , and that all other assets have equal dividend shares $(1 - s_1)/(N - 1)$. The column labelled “rel. size” shows the ratio of asset 1’s dividend share to the dividend share of any one of the other assets, $(N - 1)s_1/(1 - s_1)$. We have already seen that positive comovement and underreaction are the norm at the center of the state space. Indeed, positive comovement can occur even if asset 1 is significantly smaller than all the other assets. But for an asset to overreact, it must be significantly larger than all the other assets, and the relative amount by which it must be larger increases fairly rapidly with N .

Different calibrations deliver similar results. In the no-jump calibration, the critical values of s_1 are within 0.01 of those reported in Table S.I. The same is true if we introduce correlation between dividends in such a way that consumption volatility when all assets have equal share is held constant as N increases. On the other hand, the critical values at which comovement and overreaction take place *are* sensitive to γ . Lower γ reduces the variability of the riskless rate by more than it reduces the variability of risk premia, so underreaction and positive comovement occur over more of the simplex.

Figure S.4 shows 3D plots corresponding to the contour plots in Figure 8.

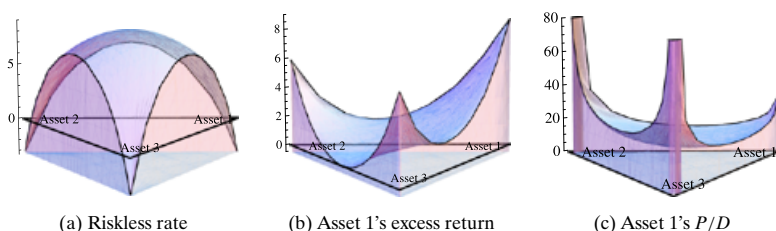


FIGURE S.4.—The riskless rate, and asset 1’s excess return and price-dividend ratio.

ADDITIONAL REFERENCE

CAMPBELL, J. Y. (1993): "Intertemporal Asset Pricing Without Consumption Data," *American Economic Review*, 83 (3), 487–512. [4]

Stanford Graduate School of Business, Stanford University, Stanford, CA 94305, U.S.A.; ian.martin@stanford.edu.

Manuscript received February, 2009; final revision received July, 2012.